Received: 2 May 2019 | Revised: 20 September 2019 | Accepted: 7 October 2019

DOI: 10.1002/jmor.21074

RESEARCH ARTICLE

JOURNAL OF morphology WILEY

Covariation between forelimb muscle anatomy and bone shape in an Australian scratch-digging marsupial: Comparison of morphometric methods

Meg L. Martin[1] | Kenny J. Travouillon[2] | Emma Sherratt[3] | Patricia A. Fleming[1] | Natalie M. Warburton[4]

[1]Environmental and Conservation Sciences, Murdoch University, Murdoch, Western Australia, Australia

[2]Department of Terrestrial Zoology, Western Australian Museum, Welshpool, Western Australia, Australia

[3]School of Biological Sciences, University of Adelaide, North Terrace, Adelaide, South Australia, Australia

[4]Medical, Molecular, and Forensic Sciences, Murdoch University, Murdoch, Western Australia, Australia

Correspondence
Meg L. Martin, Environmental and Conservation Sciences, Murdoch University, Murdoch, WA 6150, Australia.
Email: m.lane@murdoch.edu.au

Abstract

The close association between muscle and bone is broadly intuitive; however, details of the covariation between the two has not been comprehensively studied. Without quantitative understanding of how muscle anatomy influences bone shape, it is difficult to draw conclusions of the significance of many morphological traits of the skeleton. In this study, we investigated these relationships in the Quenda (*Isoodon fusciventer*), a scratch-digging marsupial. We quantified the relationships between forelimb muscle anatomy and bone shape for animals representing a range of body masses (124–1,952 g) using two-block partial least square analyses. Muscle anatomy was quantified as muscle mass and physiological cross-sectional area (PCSA), and we used two morphometric methods to characterize bone shape: seven indices of linear bone proportions, and landmarks analysis. Bone shape was significantly correlated with body mass, reflecting allometric bone growth. Of the seven bone indices, only shoulder moment index (SMI) and ulna robustness index (URI) showed a significant covariation with muscle anatomy. Stronger relationships between muscle anatomy and forelimb bone shape were found using the landmark coordinates: muscle mass and PCSA were correlated with the geometric shape of the scapula, humerus, and third metacarpal, but to a lesser extent with shape of the ulna. Overall, our data show that landmark coordinates are more sensitive than bone indices to capturing shape changes evident throughout ontogeny, and is therefore a more appropriate method to investigate covariation with forelimb muscle anatomy. Single-species studies investigating ontogeny require refined methods to accurately develop understanding of the important relationships between muscle force generation and bone shape remodeling. Landmark analyses provide such a method.

KEYWORDS

Biopedturbation, humerus, scapula, third metacarpal, two-block partial least squares, ulna

1 | INTRODUCTION

An animal's musculoskeletal system is shaped and altered as the individual grows in response to mechanical forces associated with movement (Currey, 2013). Differences in the musculoskeletal system between groups and species reflect adaptations to particular movements and behaviors, and thus also represent an animal species' ecological niche. For example, arboreal species demonstrate strong elbow, wrist, and digital flexors to meet the mechanical forces imposed by brachiation (Leischner et al., 2018). In contrast, cursorial species have proximal pelvic limb muscles enlarged and specialized for force generation, proximal thoracic limb muscles specialized for action over a large range of motion

(Williams, Wilson, Rhodes, Andrews, & Payne, 2008). For an individual animal, such relationships will also vary as the individual increases in body mass during growth, and/or changes aspects of its behavior over time.

Characteristics of behavior are particularly evident in the bony and muscular anatomy of digging mammals. In addition to the requirements for locomotion, these animals also demonstrate specializations for digging. Species that are highly specialized for scratch-digging and burrowing (semi-fossorial and fossorial animals) have enlarged muscles associated with the power stroke (i.e., humeral retractors, elbow extensors, and carpal/digital flexors) as they are required to match the mechanical resistance of the substrate they dig through (Moore, Budny, Russell, & Butcher, 2013; Warburton, Grégoire, Jacques, & Flandrin, 2013). These muscular changes are then reflected in their bony anatomy. For example, the marsupial mole (Marsupialia: Notoryctemorphia) shows some of the more extreme specializations for fossorial behavior; their forelimb bones reflect their highly-specialized digging motion of "sand-swimming" in which they constantly back-fill their burrow (Warburton, 2006). All forelimb bones of the marsupial mole show specializations: the scapula is elongated and narrow, which reflects a reduction on muscles attaching to the vertebral column to allow for more posterior rotation, while the humerus and ulna are short and robust to assist the forelimb in withstanding the large muscular force and reaction forces acting against the bone during the digging motion. These patterns are observable in extant and extinct Notoryctes (Beck, Warburton, Archer, Hand, & Aplin, 2016; Warburton, 2006). Scratch-digging mammals show similar forelimb adaptions, though in less extreme forms: shortened and robust bones, enlarged distal epicondyles, and increased bone surface areas providing increased surface area for enlarged muscle attachment (Cingulates: Milne, Vizcaíno, & Fernicola, 2009; Mustelidae: Rose, Moore, Russell, & Butcher, 2014; Tenrecoidea: Salton & Sargis, 2008; Myrmecophagidae: Sesoko et al., 2015). Such specializations of the forelimbs provide the mechanical advantage necessary for digging.

The relationship between bone shape and muscle size in vertebrates reflects the forces acting on the musculoskeletal system as the body performs motions (Currey, 2013). One measure could therefore be used to predict the other. Morphometrics and associated multivariate statistical analyses used to quantify biological shape and assess covariation largely follow two approaches (Adams, Rohlf, & Slice, 2013). First, traditional morphometrics uses linear measurements and derived ratios/indices, which are useful in assessing bony proportions. These methods are particularly suited to studying articulated structures. Second, advances in computing power have allowed rapid development of geometric morphometrics using coordinate-based methods (in two- or three-dimensions) to characterise shape; such methods are increasingly common practice for quantifying individual bone shapes (Zelditch, Swiderski, & Sheets, 2012). Understanding the relative value of each approach in the context of quantifying covariation with muscle anatomy would be helpful in guiding future work.

Unfortunately, muscles and bones are often studied separately, with quantitative studies that match these tissues being rare; the exceptions have focused on the skull, investigating bite force and feeding strategies (e.g., Cornette, Tresset, & Herrel, 2015; Fabre et al., 2018; Fabre, Andrade, Huyghe, Cornette, & Herrel, 2014; Noback & Harvati, 2015; Sella-Tunis, Pokhojaev, Sarig, O'Higgins, & May, 2018). There has been a general lack of postcranial studies, and very few studies have investigated the quantitative relationship between bones and muscles for digging mammals (e.g., Böhmer, Fabre, Herbin, Peigné, & Herrel, 2018; Warburton et al., 2013). Of those studies that have investigated interactions between muscles and bones, the majority have used linear bone measurements and associated ratios/indices to make inferences about muscle anatomy (e.g., Böhmer et al., 2018), while others have used landmark coordinates without clear extrapolation to muscle anatomy (e.g., Carlon, 2014; McCabe, Henderson, Pantinople, Richards, & Milne, 2017). Also lacking in the literature are studies that explicitly compare the two methods of assessing bone shape (indices and landmark coordinates; e.g., Bernal, 2007; Bonnan, Farlow, & Masters, 2008; Breno, Leirs, & Van Dongen, 2011).

We carried out morphometric analysis of the forelimb of the Quenda (*Isoodon fusciventer*) to quantify the relationship between the shape of forelimb long bone and associated muscle anatomy (i.e., physiological cross-sectional area; PCSA) to test the extent to which these two parameters covary. Furthermore, we test indices and landmark coordinates as methods for quantifying bone shape, to determine which method provides the better insight into muscle force production. Specifically, we predict that shape covariation will be greater between the landmark coordinates and muscle PCSA as this method captures the precise geometry of bones, and thus conveys more shape information in comparison with the bone indices.

Quenda employ their forelimbs for scratch-digging to search for subterranean food items (e.g., invertebrates, bulbs, and fungi fruiting bodies) as well as to construct short burrows and nests for shelter (Gordon & Hulbert, 1989; Long, 2009; Warburton & Travouillon, 2016). The species displays adaptations of both muscle and bone anatomy associated with scratch-digging (Warburton et al., 2013). This study builds on previous findings that showed Quenda force generation capacity (PCSA) showed differential growth between main movers of the recovery stroke and the power stroke of scratch-digging (Martin, Warburton, Travouillon, & Fleming, 2019). We therefore predicted that muscles associated with the power-stroke of digging will have disproportionate influence on shape change of the long bones. To account for allometric effects, we repeated analyses on the residuals of linear regressions of muscle forces (PCSA) and bone shape data against body mass. This study contributes to our understanding of how forelimb muscle anatomy influences bone shape, and how these structures functionally covary in a digging marsupial as a reflection of the mechanical demands of scratch-digging.

2 | MATERIALS AND METHODS

The Quenda (*Isoodon fusciventer*), formerly listed as a subspecies of Southern Brown Bandicoot (*I. obesulus fusciventer*), has recently

been raised to species level based on cranio-dental morphology and molecular data (Travouillon & Phillips, 2018). We sampled 32 Quenda specimens: 19 males (1,041 ± 667 g) and 13 females (810 ± 356 g). Males can reach larger body mass than females (males: 500-1800 g, females: 400–1,200 g; Warburton & Travouillon, 2016), although the difference in body mass in our data set was not significant (t_{32} = −1.15, p = .259). The specimens were from either Kanyana Wildlife Rehabilitation Centre, Lesmurdie, Western Australia, or opportunistically collected throughout the Perth metropolitan area (Regulation 17 licence SF010344; accidental deaths including road collisions, pool drownings, and domestic pet attack). As some specimens were often injured, forelimb bones were sometimes too badly damaged to be analyzed; consequently, the number of specimens per bone varied.

Muscles were dissected and measured for mass and PCSA; these data have been fully analyzed and published separately (Martin et al., 2019) (Table 1). Muscle mass is a representation of overall muscle size, while PCSA is a representation of maximum isometric force production for individual muscles. PCSA is generally considered a more appropriate measure of muscle force potential to interpret biological functions in correlation with skeletal morphology (Myatt et al., 2012; Thorpe, Crompton, Gunther, Ker, & McNeill, 1999).

2.1 | Morphometric analyses

The scapula, humerus, ulna and third metacarpal for each specimen were scanned using a Skyscan 1176 scanner (Bruker microCT; Centre of Microscopy, Characterization and Analysis, The University of Western

TABLE 1 List of muscles, abbreviations, and functional groups used for the study. Muscles ordered proximal to distal and colors represent muscle groups and are represented in Figures 3–6

Muscle	Abbreviation	Usage in 2b-PLS with indices	Functional group
Trapezius	Tra	-	Scapula stabilisation (SS)
Omotransversarius	OmT	-	Scapula stabilisation (SS)
Rhomboideus	Rho	-	Scapula stabilisation (SS)
Serratus ventralis	SeV	-	Scapula stabilisation (SS)
Supraspinatus	Sup	BI, SMI	Humeral protraction (HP)
Latissimus dorsi	LtD	SMI, HTRI, HCRI	Humeral retraction (HR)
Pectoralis group	Pec	BI, SMI, HTRI, HCRI	Humeral retraction (HR)
Deltoideus	Del	SMI, HTRI, HCRI	Humeral retraction (HR)
Infraspinatus	Inf	BI, SMI	Humeral retraction (HR)
Teres major	TMj	BI, SMI	Humeral retraction (HR)
Subscapularis	Sub	BI, SMI	Humeral retraction (HR)
Biceps brachii	BiB	BI, SMI, HTRI, HCRI, URI	Elbow flexion (EF)
Brachialis	Bra	BI, HTRI, HCRI, URI	Elbow flexion (EF)
Triceps brachii	TrB	BI, SMI, HTRI, HCRI, EI, IFA	Elbow extension (EE)
Anconeus	Anc	BI, EI. IFA	Elbow extension (EE)
Tensor fascia antebrachii	TFA	IFA	Elbow extension (EE)
Flexor carpi radialis	FCR	BI, EI, URI	Carpal/digital flexion (CDF)
Flexor carpi ulnaris	FCU	BI, EI, URI	Carpal/digital flexion (CDF)
Palmaris longus	PaL	BI, EI, URI	Carpal/digital flexion (CDF)
Flexor digitorum superficialis	FDS	BI, EI, URI	Carpal/digital flexion (CDF)
Flexor digitorum profundus	FDP	BI, EI, URI	Carpal/digital flexion (CDF)
Pronator teres	PrT	BI, EI, URI	Pronators (PRO)
Pronator quadratus	PrQ	URI	Pronators (PRO)
Extensor carpi radialis	ECR	BI, EI, URI	Carpal/digital extension (CDE)
Extensor digitorum communis	EDC	BI, EI, URI	Carpal/digital extension (CDE)
Extensor digitorum lateralis	EDL	BI, EI, URI	Carpal/digital extension (CDE)
Extensor carpi ulnaris	ECU	BI, EI, URI	Carpal/digital extension (CDE)
Abductor digiti I longus	AbdL	URI	Carpal/digital extension (CDE)
Supinator	Spr	BI, URI	Supinators (SUPI)

Abbreviations: BI, brachial index; EI, epicondyle index; HCRI, humerus cranial-caudal robustness index; HTRI, humerus transverse robustness index; IFA, index of fossorial ability; SMI, shoulder moment index; URI, ulna robustness index.

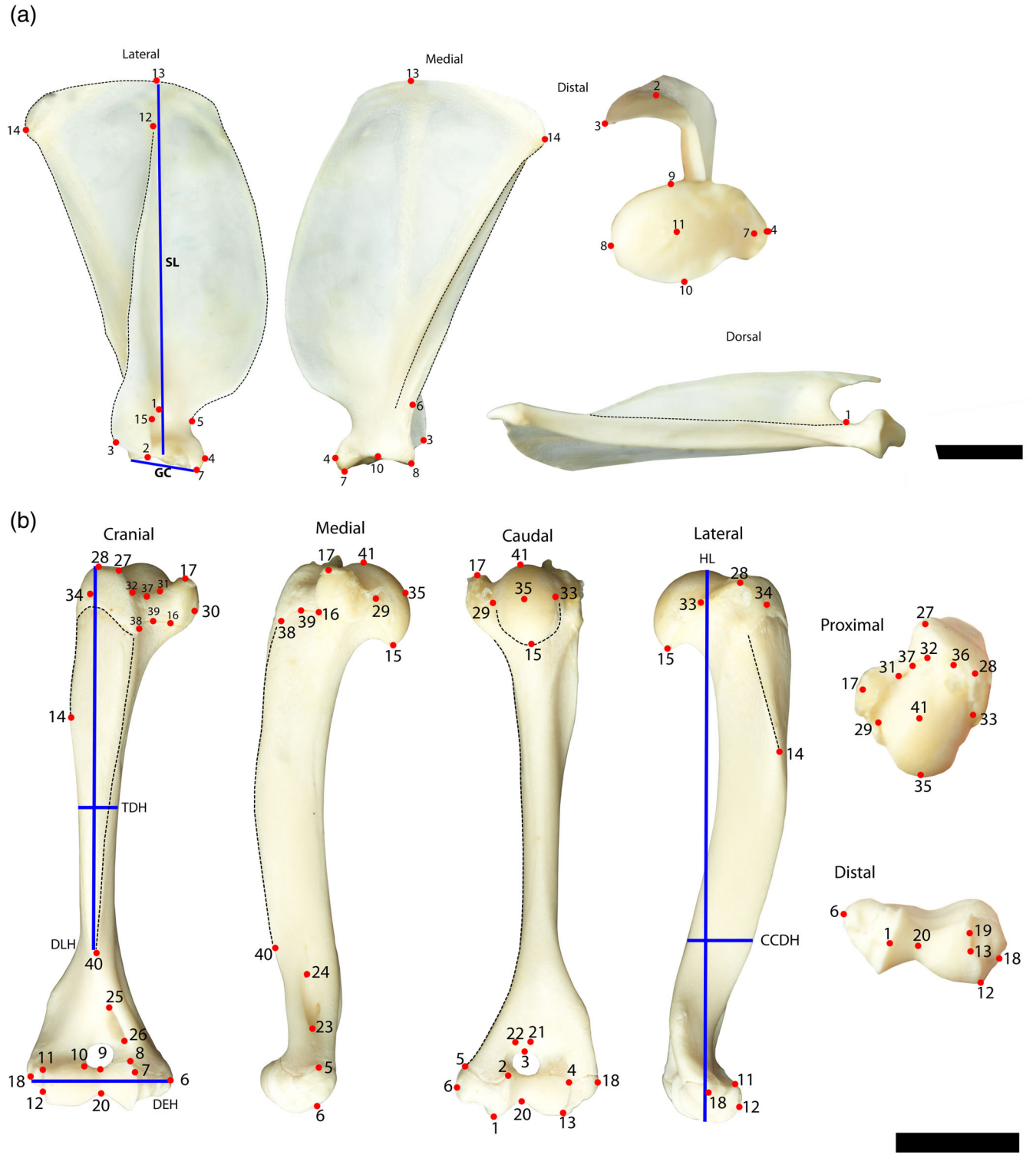

FIGURE 1 Linear measurements (soild lines) and landmarks (red points) used in analysis to quantify shape variation on the forelimb. Dashed lines represent curves of semi-sliding landmarks. (a) 15 homologous landmarks and 81 semi-sliding landmarks for the scapula, and scapular length (SL) and glenoid cavity diameter (GC) linear measurements. (b) 41 homologous landmarks and 33 semi-sliding landmarks for the humerus, and deltoid length of humerus (DLH), transverse diameter of humerus (TDH), functional humeral length (HL), cranial-caudal diameter of humerus (CCDH) linear measurements. Scale bar represents 100 mm

Australia) at a resolution of 35 μm, with a 0.2-mm aluminium filter, voltage 45 kv, and amperage 550 μA. Scans were reconstructed using the software NRecon (Burker microCT) which produces stacks of images that were visualized in CTAn (Burker microCT) as a 3D digital volume. The volumes were processed via a threshold approach to digitally dissect the bone, and surface models of the bones were exported as .ply files.

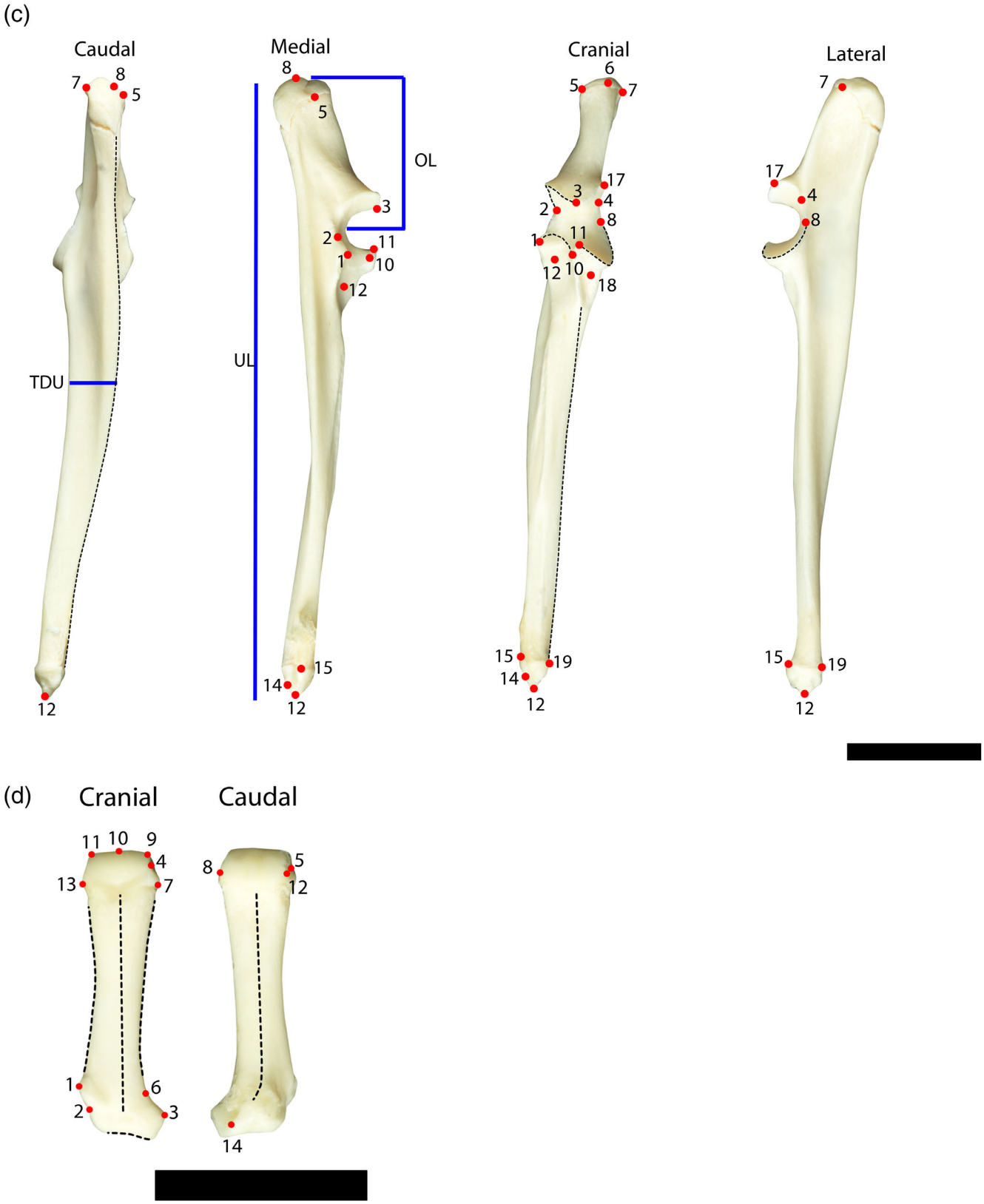

FIGURE 2 Linear measurements (solid lines) and landmarks (red points) used in analysis to quantify shape variation on the forelimb. Dashed lines represent curves of semi-sliding landmarks. (c) 19 homologous landmarks and 57 semi-sliding landmarks for the ulna, and transverse diameter of the ulna (TDU), olecranon length (OL), total ulnar length (UL) linear measurements. (d) 14 homologous landmarks and 37 semi-sliding landmarks for the third metacarpal. Scale bar represents 100 mm

2.1.1 | Indices

Seventeen linear variables of the scapula, humerus, ulna, and third metacarpal were measured on skeletal material to the nearest 0.01 mm using PES digital callipers (Figure 1 and Figure 2) which were combined to calculate seven functional indices that represent attributes of the forelimb bones and the potential mechanical efficiency for digging (Table 2). The indices have developed in the literature as means of characterizing limb specializations, primarily used to distinguish between species, and predict different styles of digging and ecology (i.e., diggers, occasional diggers, generalized, burrowers, and cursorial; Hopkins & Davis, 2009). Indices are ratios, and therefore control for size variation in the sample (Klingenberg, 2016).

2.1.2 | Landmark coordinates

The software IDAV Landmark Editor v.3.6 (Wiley et al., 2005) was used to place homologous landmarks and curves of semi-sliding landmarks to the bones (Figure 1 and Figure 2; detailed descriptions of the individual landmarks are listed in the Tables s1–S4). Landmark coordinates analyses were completed in R (R Development Core Team, 2018) using the package *geomorph* v.3.0.4 (Adams, Collyer, & Sherratt, 2018; Adams & Otárola-Castillo, 2013). Landmarks were aligned using Generalized Procrustes Superimposition to remove the effects of size, position, and orientation, leaving only shape variation (Rohlf & Slice, 1990). During Procrustes superimposition, the semi-sliding landmarks were permitted to slide along their tangent directions to minimize the Procrustes distance between specimens.

2.2 | Allometry in bone shape

In order to address potential sex differences and allometric relationships between bone shape and muscles, we used a multivariate analysis of covariance (MANCOVA) model testing bone shape (indices and landmark coordinates as dependent variables in two separate analyses) against log-transformed body mass, with sex as independent factor (implemented with function procD.lm in *geomorph*; R Development Core Team, 2018). The models were evaluated for statistical significance with Goodall's *F*-test (Goodall, 1991) using a permutation procedure (1,000 permutations).

2.3 | Covariation between forelimb muscle anatomy and bone shape

To quantify the strength of covariation between forelimb muscle anatomy (mass and PCSA) and bone shape (indices and landmark coordinates), we carried out a series of two-block partial least squares (2b-PLS) analyses (Rohlf & Corti, 2000) implemented using two.b.pls function in *geomorph*. This method identifies axes in two multivariate datasets ("blocks") that explain the covariance between them, and quantifies the degree of association between the two blocks by constructing pairs of variables that are linear combinations of the variables within each of the two blocks. The linear combinations construct new variables that account for as much of the covariation as possible between the two blocks. The results of the 2b-PLS analysis are an *r-PLS* value: the correlation coefficient between the scores of projected values from the two blocks, and an associated *p*-value: empirically calculated from the resampling procedure.

First, 2b-PLS was performed individually for the seven indices against log-transformed muscle anatomy including only muscles associated with the bone or the index (listed in Table 1); and for landmark coordinates each forelimb bone individually against log-transformed muscle anatomy. These tests examined the strength of covariation due to allometry.

TABLE 2 Description of the seven indices of digging ability used in this study

	Calculation	Description	References[a]
Brachial index (BI)	BI = (UL − OL)/HL × 100	Indication of relative distal out-lever length	4, 5
Shoulder moment index (SMI)	SMI = DLH/HL × 100:	Indication of the mechanical advantage of the pectoral muscles and deltoid to act across the shoulder joint	1, 2, 3, 4, 5
Humerus transverse robustness index (HTRI)	HTRI = TDH/HL × 100:	Indication of the robustness of the humerus	1, 2, 3, 4, 5
Humerus cranial-caudal robustness index (HCRI)	HCRI = CCDH/HL × 100	Indication of the robustness of the humerus	5
Epicondyle index (EI)	EI = DEH/HL × 100:	Indication of width available for the flexor, pronator and supinator muscles of the forearm to attach	1, 2, 3, 4, 5
Ulna robustness index (URI)	URI = TDU/(UL − OL) × 100:	Indication of the robustness of the forearm	1, 4, 5
Index of fossorial ability (IFA)	IFA = OL/(UL − OL) × 100:	Indication of mechanical advantage of the triceps in the elbow extension and is considered a good indicator of fossoriality	1, 2, 3, 4, 5

Note: Descriptions of how each related to the functional morphology of the forelimb.
Abbreviations: CCDH, cranial caudal diameter of humerus; DEH, diameter of the epicondyles; DLH, deltoid length of humerus; HL, humeral length; OL, olecranon length; TDH, transverse diameter of humerus; TDU, transverse diameter of the ulna; UL, ulnar length.
[a]References: [1](Elissamburu & de Santis, 2011), [2](Elissamburu & Vizcaíno, 2004), [3](Lagaria & Youlatos, 2006), [4](Rose et al., 2014), [5](Warburton et al., 2013).

TABLE 3 Examining allometry: MANCOVAs of the three significant indices and the four forelimb bones (landmark coordinates) shape by size (Y ~ total body mass) and sex (Y ~ total body mass*sex)

	Df	*SS*	*MS*	R^2	*F*	*p*
a. Indices						
Brachial index (BI) shape						
Log(body mass)	1	167.67	167.67	0.23	8.64	0.011
Sex	1	10.48	10.48	0.01	0.54	0.437
Log(body mass) × sex	1	1.13	1.13	<0.01	0.06	0.748
Residuals	28	543.40	19.41			
Total	31	722.67				
Humerus cranial-caudal robustness index (HCRI) shape						
Log(body mass)	1	25.40	25.40	0.43	25.19	0.001
Sex	1	4.94	4.94	0.08	4.90	0.006
Log(body mass) × sex	1	0.11	0.11	<0.01	0.11	0.644
Residuals	28	28.23	1.01			
Total	31	58.68				
Index of fossorial ability (IFA) shape						
Log(body mass)	1	66.10	66.10	0.23	8.73	0.007
Sex	1	0.58	0.58	<0.01	0.08	0.765
Log(body mass) × sex	1	10.06	10.06	0.04	1.33	0.185
Residuals	28	211.95	7.57			
Total	31	288.79				
b. Landmark data						
Scapular landmark shape						
Log(body mass)	1	0.01	0.01	0.14	2.43	0.007
Sex	1	0.01	0.01	0.07	1.24	0.130
Log(body mass) × sex	1	<0.01	<0.01	0.06	1.12	0.161
Residuals	13	0.05	<0.01			
Total	16	0.06				
Humeral landmark shape						
Log(body mass)	1	0.01	0.01	0.16	5.09	0.001
Sex	1	<0.01	<0.01	0.03	1.11	0.149
Log(body mass) × sex	1	<0.01	<0.01	0.02	0.74	0.515
Residuals	26	0.05	<0.01			
Total	29	0.07				
Ulnar landmark shape						
Log(body mass)	1	<0.01	<0.01	0.08	2.32	0.042
Sex	1	<0.01	<0.01	0.02	0.56	0.834
Log(body mass) × sex	1	<0.01	<0.01	0.04	1.04	0.297
Residuals	26	0.05	<0.01			
Total	29	0.06				
Third landmark metacarpal shape						
Log(body mass)	1	0.01	0.01	0.09	2.91	0.001
Sex	1	<0.01	0.01	0.05	1.61	0.027
Log(body mass) × sex	1	<0.01	<0.01	0.03	0.93	0.352
Residuals	28	0.09	<0.01			
Total	31	0.10				

Note: Degrees of freedom (*Df*), sums of squares (*SS*), coefficient of determination (R^2), and the *F* ratio and associated *p*-value. Bold values indicate *p*-values less than 0.05. Remaining indices ($p > 0.05$) can be found in Table S5.

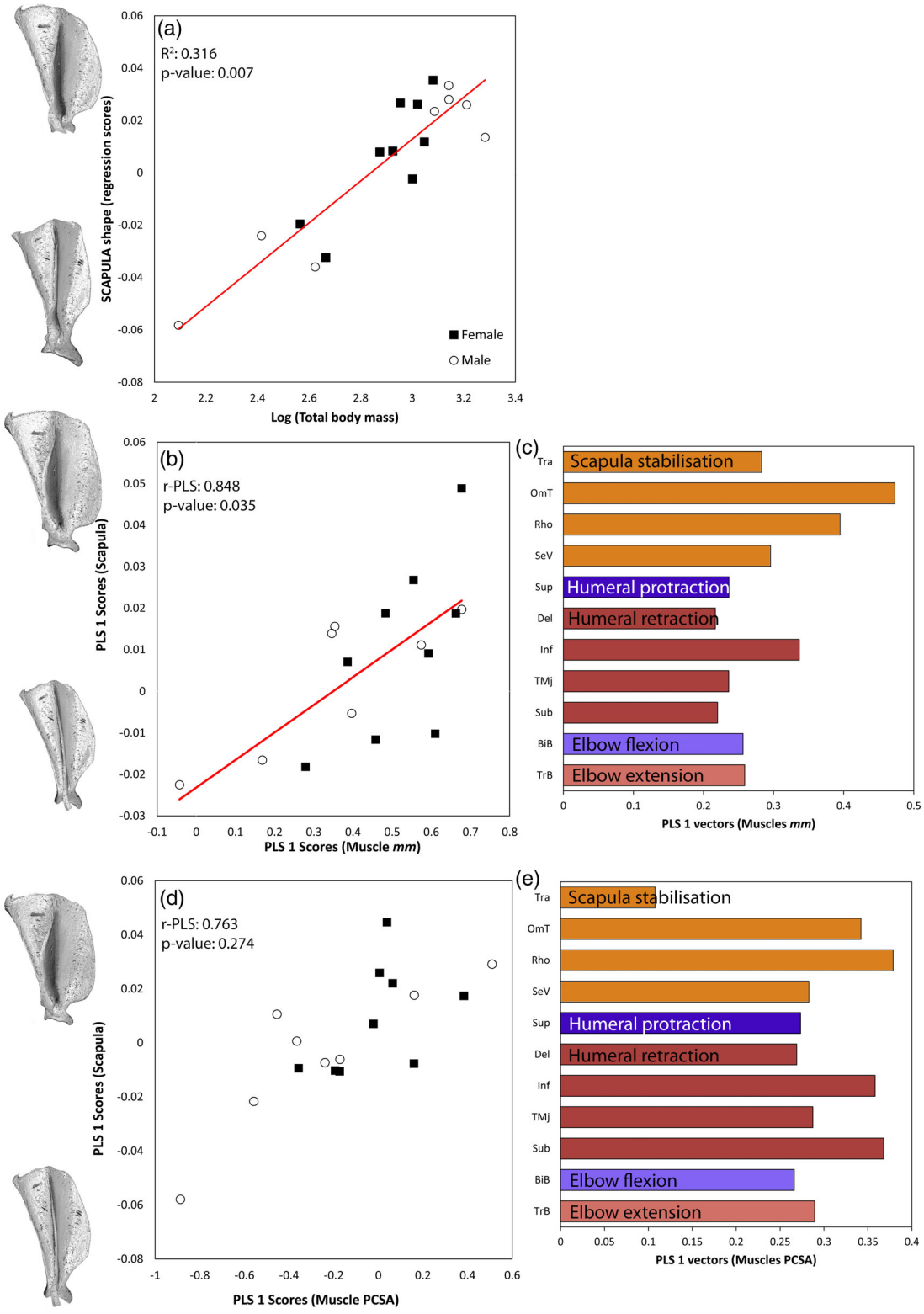

FIGURE 3 Results of the morphometric covariation analysis for the scapula (a–e) using landmark coordinates. Results of the multivariate regression which visualizes the patterns between size and shape (allometry) (a) and the results of the two-block partial least square (2b-PLS) between the forelimb landmark coordinates and the muscle mass (b,c) and PCSA (d,e) of the associated forelimb muscles. Residual values of the landmark coordinates and muscle anatomy were used to control for the size component. Scatter plots of the first PLS axis describing the shape covariation between scapula and the PCSA of the forelimb muscles (b,d). Forelimb bone shapes associated with each minimum and maximum of covariation are illustrated on the axis. Muscle loadings associated with the forelimb bone shape covariation are represented in the histogram (c,e). Muscles are ordered from proximal to distal and color-coded by functional group (Table 1). In this and further figures, there are varying number of individuals between the bones due to some bones being too badly damaged to be analyzed

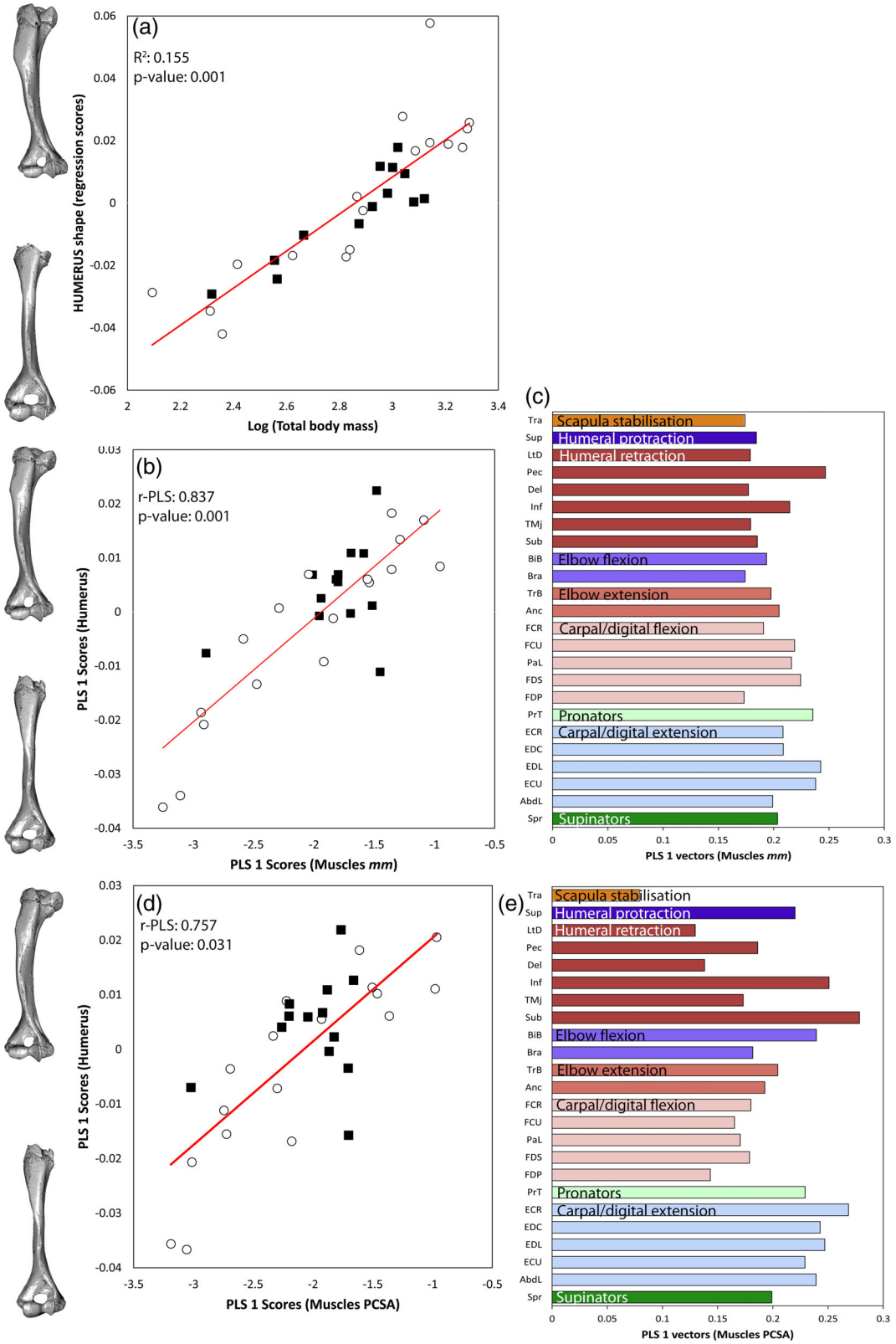

FIGURE 4 Results of the analysis for the humerus (a–e) using landmark coordinates. Format as per Figure 3

Second, to exclude the effects of allometry (Klingenberg, 2016), the above analyses were repeated using residuals calculated from linear regressions of the bone shape data (indices, landmarks) and muscle anatomy (mass and PCSA) against log-transformed body mass. These were calculated using resid(lm) (R Development Core Team, 2018) for each indices and muscle anatomy, and using procD.lm in *geomorph* for landmark shape data.

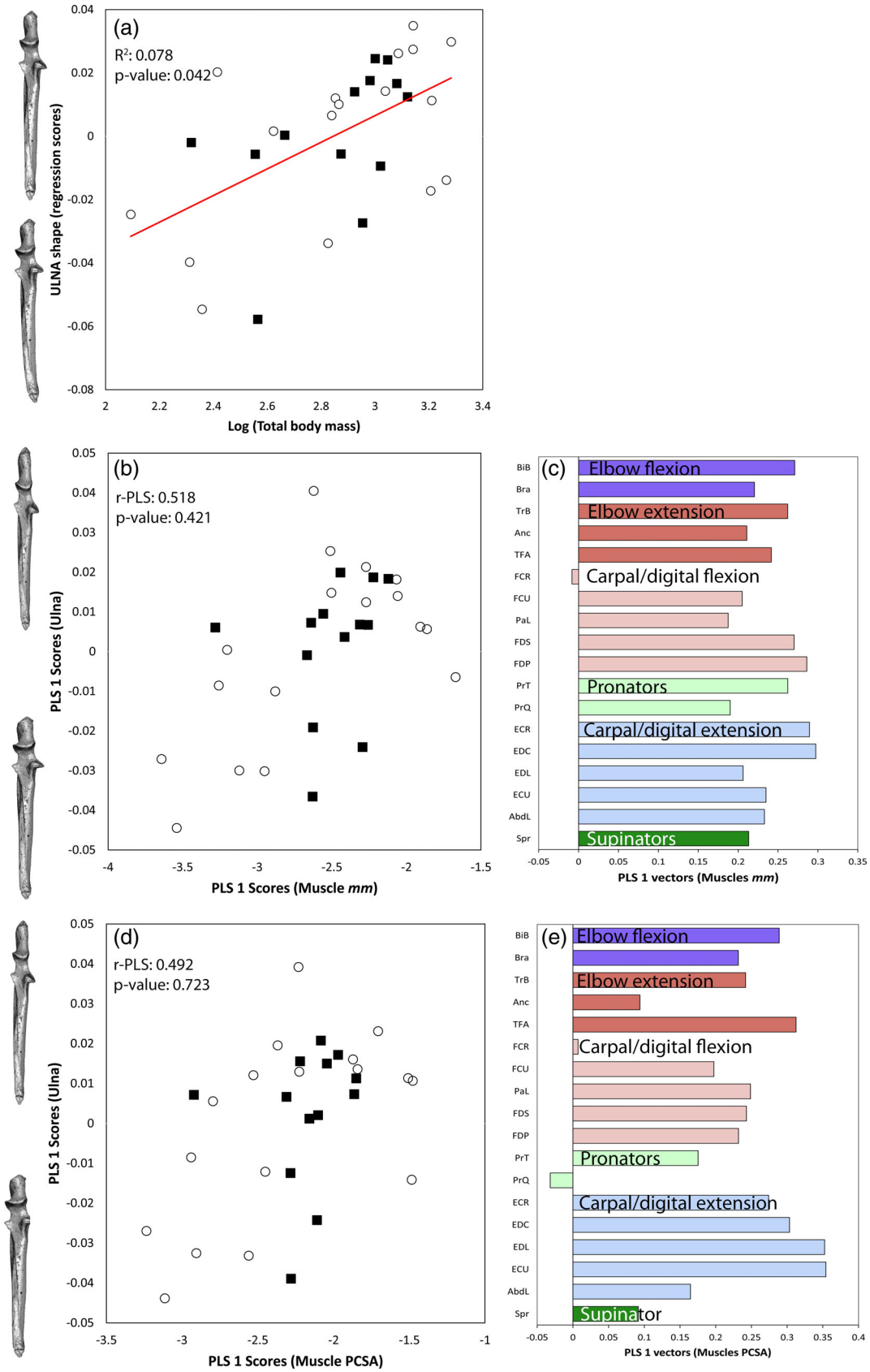

FIGURE 5 Results of the analysis for the ulna (a–e) using landmark coordinates. Format as per Figure 3

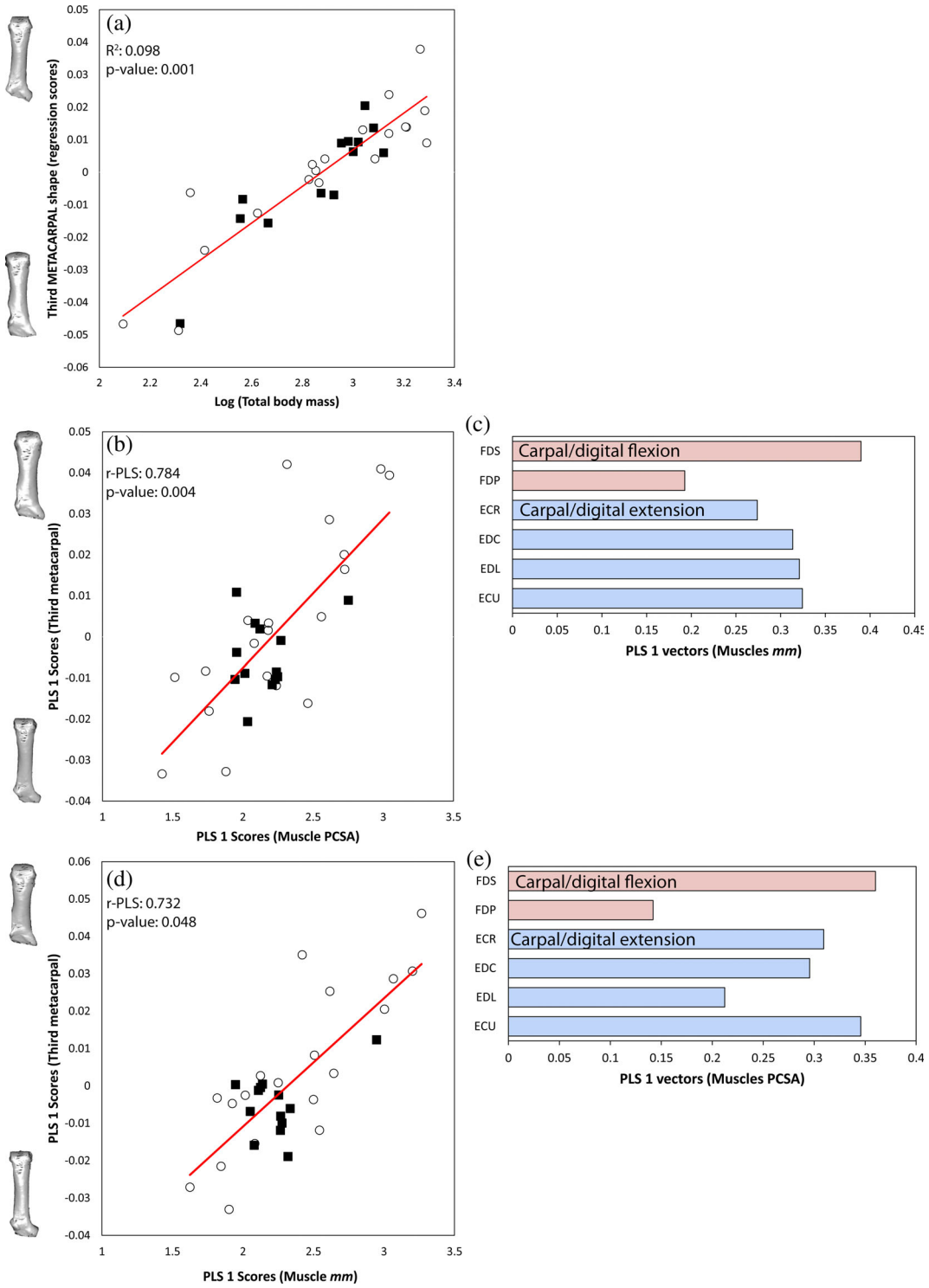

FIGURE 6 Results of the analysis for the third metacarpal (a–e) using landmark coordinates. Format as per Figure 3

3 | RESULTS

3.1 | Allometry in bone shape

3.1.1 | Indices

Of the seven indices, only three showed significant allometric associations with body mass (Table 3). The brachial index (BI), humerus cranial-caudal robustness index (HCRI), and the index of fossorial ability (IFA) were associated with body mass, while the remaining four indices showed no significant association. HCRI was the only index to show an interaction for sex, although there was no significant interaction term between body mass and sex, indicating that the allometric slopes between males and females were the same.

3.1.2 | Landmark coordinates

MANCOVA showed significant allometric associations between body mass and bone shapes for the landmark coordinates for all four bones (Table 3). Body mass explained between 8 and 16% of the shape variation, while sex explained less than 7% of the shape variation (Figure 3a, 4a, 5a, 6a). Allometry in scapular shape was primarily evident in the cranial and caudal borders as well as the shape and relative size of the glenoid cavity and coracoid process. The humerus primarily changed in the deltopectoral crest and the epicondyles. Shape variation in the ulna was primarily in the trochlear notch. The third metacarpal showed minimal shape change to the proximal end of the bone, although this shape change was strongly associated with body mass.

Only the third metacarpal showed a significant sex difference the change of shape (4.8% of variance). The interaction terms between body mass and sex for all four bones were not significant, which indicates that allometric slopes did not differ between the sexes. Due to these negligible sex differences, the sexes were pooled for all further analyses.

3.2 | Covariation between bone shape and forelimb muscle anatomy

3.2.1 | Indices

Four of the bone shape indices—BI, HTRI (the humerus transverse robustness index), HCRI and IFA—showed significant covariation associated with muscle mass; three of these—BI, HCRI, IFA—were those indices also correlated with body mass. Two indices covaried with muscle PCSA: HCRI, SMI (shoulder moment index; Table 4). When allometric relationships were removed, only two indices retained significant covariation: URI (ulna robustness index) covaried with muscle mass (largely the FCR [flexor carpi radialis], and FDS [flexor digitorum superficialis]), while SMI covaried with muscle PCSA (largely driven by the Inf [infraspinatus], and LtD [latissimus dorsi]).

3.2.2 | Landmark coordinates

Covariation between the landmark coordinates and forelimb muscle anatomy (both mass and PCSA) was evident for the scapula, humerus, and third metacarpal; no covariation was seen between the ulnar shape and muscle anatomy. When the influence of body mass was removed (analysis of residuals), covariance remained significant in all bones except between scapula shape and muscle PCSA (Table 4).

Variation in muscle anatomy was associated with changes in the scapular shape at the cranial and caudal borders, as well as the scapular spine, and therefore change in shape of the infraspinous, supraspinous, and subscapular fossae (Figure 3b,d). Scapular shape varied with mass of the omotransversarius (OmT), rhomboideus (Rho), and infraspinatus (Inf) (Figure 3c). Muscle PCSA varied additionally with the subscapularis (Sub) (Figure 3e) although this association was not significant when using the residual data. Individuals with more massive muscles and greater PCSA values had a scapula with a relatively more rounded and wide supraspinous fossa.

For the humerus, variation in muscle anatomy was associated with changes in the humeral capitulum, lesser tuberosity and the pectoral ridge, and therefore changes in articulation at the elbow joint, and muscle origin and insertion points (Figure 4b,d). Humeral shape varied with mass of the carpal/digital extensors, pectoralis (Pec), and the pronator teres (PrT) (Figure 4c). Humeral shape varied with PCSA of the subscapularis (Sub), infraspinatus (Inf), and extensor carpi radialis (ECR) (Figure 4e). Individuals with more massive muscles and greater PCSA values had a larger lesser tuberosity and a rotated/bowed humeral shaft.

There was no significant covariation between muscle anatomy (mass and PCSA) and ulnar shape (Figure 5b,d). The shape change evident in the ulna was concentrated at the trochlear notch, coronoid process, and olecranon, and therefore changes in the articulation surface and the insertion for triceps brachii.

For the third metacarpal, variation in muscle anatomy was associated with changes in the proximal end shape and shaft robustness (Figure 6b,d), and therefore changes in the articulation surface with the carpal bones. Shape of the third metacarpal varied with mass of the flexor digitorum superficialis (FDS), extensor carpi ulnaris (ECU), and extensor digitorum lateralis (EDL). Shape of the third metacarpal varied with PCSA (Figure 6e) of flexor digitorum superficialis (FDS) and extensor carpi radialis (ECR). Individuals with more massive muscles and greater PCSA values had a more robust metacarpal shaft.

4 | DISCUSSION

Few studies in the literature have assessed the relationship between muscle anatomy and bones, and rarely have quantified the covariation of the forelimb muscle anatomy with bone shape (Cornette, Baylac, Souter, & Herrel, 2013; Fabre et al., 2014, 2018). We present the first study to demonstrate strong quantitative relationships between muscle anatomy and bone shape in limbs of a digging mammal. Independent of the allometric relationships with body mass, we identified strong correlations between muscle anatomy (mass and PCSA) and forelimb bone shape (quantified using landmark coordinates) in the Quenda. This study is therefore an important step to understand how the musculoskeletal system functions, and can be used to formulate questions concerning the functional significance of morphological traits in the forelimb.

4.1 | Sex differences in bone shape change

Quenda are sexually dimorphic in body mass (Warburton & Travouillon, 2016) and we therefore predicted that there may be some sex differences in forelimb musculature or bone shape. Despite these differences, we previously identified that Quenda forelimb muscle anatomy (muscle mass, PCSA, and fiber length) showed no significant difference between the sexes (Martin et al., 2019). Furthermore, there were only minor sex differences in a single forelimb bone in the

TABLE 4 Results of the two-block partial least square (2b-PLS) analyses using (a) indices and (b) landmark coordinates

		Raw data				Residual values			
		LOG MM		LOG PCSA		MM		PCSA	
	N	r-PLS	*p*	r-PLS	*p*	r-PLS	*p*	r-PLS	*p*
a. Indices									
Brachial index	32	**0.501**	**0.011**	0.304	0.176	0.388	0.161	0.189	0.645
Shoulder moment index	32	0.281	0.122	**0.469**	**0.016**	0.397	0.055	**0.450**	**0.035**
Humerus transverse robustness index	32	**0.625**	**0.001**	0.219	0.435	0.295	0.239	0.136	0.837
Humerus cranial-caudal robustness index	32	**0.702**	**0.001**	**0.507**	**0.011**	0.337	0.123	0.367	0.089
Epicondyle index	32	0.258	0.216	0.249	0.362	0.194	0.589	0.287	0.275
Ulna robustness index	32	0.217	0.308	0.254	0.329	**0.518**	**0.024**	0.222	0.497
Index of fossorial ability	32	**0.472**	**0.006**	0.305	0.142	0.234	0.401	0.160	0.606
b. Landmark coordinates									
Scapula	17	**0.875**	**0.006**	**0.860**	**0.014**	**0.848**	**0.035**	0.763	0.274
Humerus	30	**0.880**	**0.001**	**0.866**	**0.001**	**0.837**	**0.001**	**0.757**	**0.031**
Ulna	30	0.568	0.156	0.567	0.172	0.518	0.421	0.492	0.723
Third metacarpal	32	**0.901**	**0.001**	**0.894**	**0.001**	**0.784**	**0.004**	**0.732**	**0.048**

Note: Columns show analyses for raw muscle mass and muscle PCSA data (left hand block; log-transformed values for the indices and associated muscle anatomy) and then residual data (right hand block). Values shown are the r-PLS (correlation coefficient between the scores of the indices and muscle data) and associated *p* value. Bold values indicate a significant relationship.

Quenda in the present study; the third metacarpal showed shape differences between the sexes, with males having a smaller, less elongated proximal end. These minor differences in bone shape development, which were likely to be driven by body mass and associated forelimb muscle anatomy, were unlikely to result in major functional differences in forelimb mechanics between males and females.

4.2 | Indices associated with body mass and muscle anatomy

The indices are ratios of the forelimb bones and represent relative proportions that are commonly used to determine locomotion and digging ability (Lagaria & Youlatos, 2006; Rose et al., 2014). While typically used to distinguish between species of differing digging, climbing and running abilities (Hopkins & Davis, 2009), these indices are rarely used for single-species ontogenetic studies. Since the ratio of bone proportions within one species likely exhibits less variability (intraspecific variation) compared with the large variability evident between species (interspecific variation), it was unsurprising that the seven bone indices showed little association with muscle anatomy in this ontogenetic study. However, the BI, HCRI, and IFA all increased with body mass in the Quenda, suggesting increased mechanical adaptation for digging as individuals grow.

The BI reflects the relative distal out-lever length and therefore mechanical leverage able to be applied across the whole limb. Throughout the literature, semi-fossorial species often show small values for the BI (Vizcaíno, Farina, & Mazzetta, 1999; Vizcaíno & Milne, 2002). BI increased with body mass in the Quenda, which was unexpected as digging species generally show relatively shorter forearms (Warburton et al., 2013).

Greater values for the two humeral robustness indices (HTRI or HCRI) is a common finding for digging mammals (Elissamburu & de Santis, 2011; Lagaria & Youlatos, 2006). Digging mammals that employ a sprawled and abducted limb during humeral rotation digging, such as echidnas (Tachyglosidae) and moles (Talpidae) (Barnosky, 1981; Hopkins & Davis, 2009), have an increased robustness in the transverse axis. By contrast, the HCRI (rather than HTRI) increased significantly with body mass in Quenda. These animals scratch-dig in an cranial-caudal plane (parasagittal), and therefore forces are concentrated in this axis (Warburton et al., 2013). The HCRI therefore captures the ability of the humerus to resist the high bending loads in this plane.

Lastly, of all the indices, IFA is reported to be the best predictor of fossorial ability (Elissamburu & Vizcaíno, 2004; Lagaria & Youlatos, 2006; Rose et al., 2014; Vizcaíno et al., 1999; Vizcaíno & Milne, 2002; Warburton et al., 2013). It is likely that IFA increases with body mass to increase the mechanical advantage of the triceps and elbow extensor muscles.

Few indices also showed covariation with both the residual muscle masses (URI) and PCSA (SMI). For URI, robustness of the ulna is potentially driven by antebrachium muscle mass. SMI covaried with muscle PCSA and showed shape change in the deltoid and pectoral ridge, which is reasonable as SMI represents the mechanical advantage of the pectoral and deltoid muscles across the shoulder. Few of the indices showed significant covariation with muscle anatomy, and indices therefore show limited use for predicting muscle anatomy in the forelimb.

4.3 | Landmark coordinates associated with body mass and muscle anatomy

The shape of all four forelimb bones of the Quenda changed with allometry and showed strong covariation with forelimb muscle mass and PCSA. Although the strongest relationships were exhibited for body mass, even the residual muscle and bone shape data showed significant relationships. The minimal difference between the strength of covariation calculated from log-transformed muscle anatomy and the residual muscle anatomy suggests that the association of muscle on bone shape is not just associated with allometry, but other factors also contribute.

In response to both increasing body mass and increasing muscularity, the scapula became more rounded, showed an increase in surface area (specifically infraspinous and supraspinous fossae), and widening of the acromion. The infraspinatus and supraspinatus drove this shape change and their large fleshy origins were likely to be a stronger influence on scapular shape compared with the influence of discrete or tendinous insertions shown by other muscles. The broad scapula seen in the Quenda is commonly seen in digging mammals (Hildebrand, 1985; Moore et al., 2013; Rose et al., 2014) and assists in stabilizing the shoulder by increasing surface area for the rotator cuff muscles, increasing force output while digging (Argot, 2001; Jenkins, 1973; Warburton et al., 2013).

Allometry with body mass and covariation with muscle anatomy showed the humerus became more robust (wider humeral shaft) with an increased pectoral ridge and lesser tuberosity, while the capitulum decreased in relative size. Larger specimens had relatively smaller distal joints, a pattern that has also been observed for extant and fossil armadillos (order Cingulata; Milne et al., 2009) and has been attributed to allometric principles, in that the surface area of bone increases in proportion to the square of the length increase. Different muscles covaried with humeral shape for the analyses of muscle mass or PCSA measures, suggesting that muscle size and force production influence humeral shape differently. Rotation of the pectoral ridge would be driven by an increase in the pectoralis muscle mass and by the distal insertion of the pectoralis, an observation that has been noted previously (Warburton et al., 2013). Enlarged deltopectoral ridges are associated with digging (Milne et al., 2009) as well as a large lesser tuberosity, which allows for increased surface area for the subscapularis to stabilize the shoulder joint (Argot, 2001).

Shape of the ulna showed the weakest association with body mass and muscle anatomy, suggesting that there was substantial variation in ulnar shape, which did not strongly reflect ontogeny. The patterns that were observed align with previous studies showing that digging species develop a deeper concave trochlea surface to stabilize the elbow joint (Rose et al., 2014; Sesoko et al., 2015) and limit rotation in the elbow (Andersson, 2004; Argot, 2001; Jenkins, 1973). Interestingly, the ulna robustness index (URI) significantly covaried with muscle mass; therefore, the URI may be better than landmark coordinates in representing muscles around the ulna.

The minimal shape change in proximal end of the third metacarpal bone was strongly associated with body mass and muscle anatomy. Digging mammals have relatively short and robust metacarpals with elongated claws to provide great out-forces for digging (Hildebrand, 1985; Moore et al., 2013; Salton & Sargis, 2008). All the forces generated throughout the limb are concentrated into the metacarpals and claws to cut through compact soil (Rose et al., 2014). Therefore, the metacarpals would be subject to large selective pressures. This may explain the strong patterns we observed, despite little obvious shape change.

4.4 | Comparison of indices and landmark coordinates reveals the strengths and limitations of both methods

Indices were designed to be a proxy of fossorial ability across a wide variety of taxa (Hopkins & Davis, 2009) using large sample sizes. We found that indices were largely unable to distinguish small changes in the forelimb that occur in an ontogenetic series, probably because many of the changes in the bones are not captured in the linear measurements (Zelditch, Swiderski, & Sheets, 2004). Compared with bone indices, Quenda bone shape captured as three-dimensional landmarks more strongly covaried with muscle anatomy. Landmark and semi-sliding landmarks allow for detailed comparison (Bernal, 2007; Breno et al., 2011; Maderbacher et al., 2008), and the landmark coordinate method is therefore the most suitable to represent/act as a proxy for muscle anatomy in an ontogenetic study. Our data was collected through 3D digital methods (micro-CT); however, landmarking is also possible from photographs (2D) which is an inexpensive and time efficient method of landmarking. Arguably, 2D and 3D produce similar results (e.g., Buser, Sidlauskas, & Summers, 2018; Cardini, 2014).

5 | CONCLUSIONS

We present the first study to show a strong association between muscle anatomy and bone shape irrespective of their inherent allometric correlations with body mass. Allometry with body mass was a large driver of bone shape, but we also identify relationships between muscle anatomy (mass and PCSA) that determined bone shape in the Quenda. Notably, muscles that were drivers on the bone shape were shoulder stabilisers and humeral retractors (main movers in the power stroke of digging), vital for generating large out-forces and pulling the forelimbs horizontally against the resistance of the soil in this digging species. Our results show that bone shape (3D landmarks) can be a good proxy for muscle anatomy, and bone shape analysis could therefore be used in the future for reconstructions of extinct species.

ACKNOWLEDGMENTS

The authors acknowledge the facilities, and the scientific and technical assistance of the National Imaging Facility at the Centre for Microscopy, Characterisation & Analysis, The University of Western Australia, a facility funded by the University, State and Commonwealth Governments. The authors also thank Kanyana Wildlife

Rehabilitation Centre for access to specimens. This study was carried out with the technical support at Murdoch University, and we thank Diana Nottle, Zsa Zsa Wong, and Joe Hong for their assistance. Financial support was provided by Murdoch University.

CONFLICT OF INTEREST

We have no competing interests to declare.

AUTHOR CONTRIBUTIONS

M.L.M. collect specimens, carried out all scanning and processing of specimens, landmarked all the specimens, undertook statistical analysis, and drafted the manuscript. K.J.T. drafted the manuscript, ES assisted in statistical analysis and drafted the manuscript, P.A.F. assisted in statistical analysis and drafted the manuscript, and N.M.W. collected specimens and drafted the manuscript. All authors contributed to the experimental design and gave final approval for publication.

ORCID

Meg L. Martin https://orcid.org/0000-0003-4924-309X
Kenny J. Travouillon https://orcid.org/0000-0003-1734-4742
Emma Sherratt https://orcid.org/0000-0003-2164-7877
Patricia A. Fleming https://orcid.org/0000-0002-0626-3851
Natalie M. Warburton https://orcid.org/0000-0002-8498-3053

REFERENCES

Adams, D. C., Collyer, M. L., & Sherratt, E. (2018). *Geomorph: Software for Geometric Morphometric Analyses. R Package Version 3.0.4*. Retrieved from http://cran.r-project.org/web/packages/geomorph/index.html.

Adams, D. C., & Otárola-Castillo, E. (2013). Geomorph: An r package for the collection and analysis of geometric morphometric shape data. *Methods in Ecology and Evolution*, *4*(4), 393–399. https://doi.org/10.1111/2041-210X.12035

Adams, D. C., Rohlf, F. J., & Slice, D. E. (2013). A field comes of age: Geometric morphometrics in the 21st century. *Hystrix, the Italian Journal of Mammalogy*, *24*(1), 7–14. https://doi.org/10.4404/hystrix-24.1-6283

Andersson, K. I. (2004). Elbow-joint morphology as a guide to forearm function and foraging behaviour in mammalian carnivores. *Zoological Journal of the Linnean Society*, *142*(1), 91–104. https://doi.org/10.1111/j.1096-3642.2004.00129.x

Argot, C. (2001). Functional-adaptive anatomy of the forelimb in the didelphidae, and the paleobiology of the paleocene marsupials *Mayulestes ferox* and *Pucadelphys andinus*. *Journal of Morphology*, *247*(1), 51–79. https://doi.org/10.1002/1097-4687(200101)247:1<51::AID-JMOR1003>3.0.CO;2-%23

Barnosky, A. D. (1981). A skeleton of Mesoscalops (Mammalia, Insectivora) from the Miocene deep river formation, Montana, and a review of the Proscalopid moles: Evolutionary, functional, and stratigraphic relationships. *Journal of Vertebrate Paleontology*, *1*(3/4), 285–339. https://doi.org/10.1080/02724634.1981.10011904

Beck, R. M. D., Warburton, N. M., Archer, M., Hand, S. J., & Aplin, K. P. (2016). Going underground: Postcranial morphology of the early Miocene marsupial mole *Naraboryctes philcreaseri* and the evolution of fossoriality in notoryctemorphians. *Memoirs of Museum Victoria*, *74*, 151–171. https://doi.org/10.24199/j.mmv.2016.74.14

Bernal, V. (2007). Size and shape analysis of human molars: Comparing traditional and geometric morphometric techniques. *Journal of Comparative Human Biology*, *58*(4), 279–296. https://doi.org/10.1016/j.jchb.2006.11.003

Böhmer, C., Fabre, A.-C., Herbin, M., Peigné, S., & Herrel, A. (2018). Anatomical basis of differences in locomotor behaviour in martens: A comparison of the forelimb musculature between two sympatric species of *Martes*. *The Anatomical Record*, *301*(3), 449–472. https://doi.org/10.1002/ar.23742

Bonnan, M. F., Farlow, J. O., & Masters, S. L. (2008). Using linear and geometric morphometrics to detect intraspecific variability and sexual dimorphism in femoral shape in *Alligator mississippiensis* and its implications for sexing fossil Archosaurs. *Journal of Vertebrate Paleontology*, *28*(2), 422–431. https://doi.org/10.1671/0272-4634(2008)28[422:ULAGMT]2.0.CO;2

Breno, M., Leirs, H., & Van Dongen, S. (2011). Traditional and geometric morphometrics for studying skull morphology during growth in *Mastomys natalensis* (Rodentia: Muridae). *Journal of Mammalogy*, *92*(6), 1395–1406. https://doi.org/10.1644/10-MAMM-A-331.1

Buser, T. J., Sidlauskas, B. L., & Summers, A. P. (2018). 2D or not 2D? Testing the utility of 2D vs. 3D landmark data in geometric morphometrics of the sculpin subfamily Oligocottinae (Pisces; Cottoidea). *The Anatomical Record*, *301*(5), 806–818. https://doi.org/10.1002/ar.23752

Cardini, A. (2014). Missing the third dimension in geometric morphometrics: How to assess if 2D images really are a good proxy for 3D structures? *Hystrix, the Italian Journal of Mammalogy*, *25*(2), 73–81.

Carlon, B. (2014). *Functional limb morphology of extinct carnivores Smilodon fatalis, Panthera atrox, and Canis dirus based on comparisons with four extant felids and one extant canid*. (Doctor of Philosophy). Northern Illinois University.

Cornette, R., Baylac, M., Souter, T., & Herrel, A. (2013). Does shape covariation between the skull and the mandible have functional consequences? A 3D approach for a 3D problem. *Journal of Anatomy*, *223*(4), 329–336. https://doi.org/10.1111/joa.12086

Cornette, R., Tresset, A., & Herrel, A. (2015). The shrew tamed by Wolff's law: Do functional constraints shape the skull through muscle and bone covariation? *Journal of Morphology*, *276*(3), 301–309. https://doi.org/10.1002/jmor.20339

Currey, J. D. (2013). *Bones: Structure and mechanics*. Princeton, New Jersey: Princeton University Press.

Elissamburu, A., & de Santis, L. (2011). Forelimb proportions and fossorial adaptations in the scratch-digging rodent Ctenomys (Caviomorpha). *Journal of Mammalogy*, *92*(3), 683–689. https://doi.org/10.1644/09-mamm-a-113.1

Elissamburu, A., & Vizcaíno, S. F. (2004). Limb proportions and adaptations in caviomorph rodents (Rodentia: Caviomorpha). *Journal of Zoology*, *262*(02), 145–159. https://doi.org/10.1017/S0952836903004485

Fabre, A.-C., Andrade, D. V., Huyghe, K., Cornette, R., & Herrel, A. (2014). Interrelationships between bones, muscles, and performance: Biting in the lizard *Tupinambis merianae*. *Evolutionary Biology*, *41*(4), 518–527. https://doi.org/10.1007/s11692-014-9286-3

Fabre, A.-C., Perry, J. M. G., Hartstone-Rose, A., Lowie, A., Boens, A., & Dumont, M. (2018). Do muscles constrain skull shape evolution in Strepsirrhines? *The Anatomical Record*, *301*(2), 291–310. https://doi.org/10.1002/ar.23712

Goodall, C. (1991). Procrustes methods in the statistical analysis of shape. *Journal of the Royal Statistical Society: Series B (Methodological)*, *53*(2), 285–321.

Gordon, G., & Hulbert, A. J. (1989). Peramelidae. In D. W. Walton & B. J. Richardson (Eds.), *Fauna of Australia. Mammalia* (Vol. 1B, pp. 603–624). Canberra: Australian Government Publishing Service.

Hildebrand, M. (1985). Digging of quadrupeds. In M. Hildebrand, D. M. Bramble, K. F. Liem, & B. D. Wake (Eds.), *Functional vertebrate*

morphology (pp. 89–109). Cambridge, MA: The Blknap Press of Harvard Univeristy Press.

Hopkins, S. S. B., & Davis, E. B. (2009). Quantitative morphological proxies for fossoriality in small mammals. *Journal of Mammalogy*, *90*(6), 1449–1460. https://doi.org/10.1644/08-mamm-a-262r1.1

Jenkins, F. A. (1973). The functional anatomy and evolution of the mammalian humero-ulnar articulation. *American Journal of Anatomy*, *137*(3), 281–297. https://doi.org/10.1002/aja.1001370304

Klingenberg, C. P. (2016). Size, shape, and form: Concepts of allometry in geometric morphometrics. *Development Genes and Evolution*, *226*(3), 113–137. https://doi.org/10.1007/s00427-016-0539-2

Lagaria, A., & Youlatos, D. (2006). Anatomical correlates to scratch digging in the forelimb of European ground squirrels (*Spermophilus citellus*). *Journal of Mammalogy*, *87*(3), 563–570. https://doi.org/10.2307/4094514

Leischner, C. L., Crouch, M., Allen, K. L., Marchi, D., Pastor, F., & Hartstone-Rose, A. (2018). Scaling of primate forearm muscle architecture as it relates to locomotion and posture. *The Anatomical Record*, *301*(3), 484–495. https://doi.org/10.1002/ar.23747

Long, K. (2009). Burrowing bandicoots—An adaptation to life in a fire-prone environment? *Australian Mammalogy*, *31*(1), 57–59. https://doi.org/10.1071/AM08107

Maderbacher, M., Bauer, C., Herler, J., Postl, L., Makasa, L., & Sturmbauer, C. (2008). Assessment of traditional versus geometric morphometrics for discriminating populations of the *Tropheus moorii* species complex (Teleostei: Cichlidae), a Lake Tanganyika model for allopatric speciation. *Journal of Zoological Systematics and Evolutionary Research*, *46*(2), 153–161. https://doi.org/10.1111/j.1439-0469.2007.00447.x

Martin, M. L., Warburton, N., Travouillon, K. J., & Fleming, P. A. (2019). Mechanical similarity across ontogeny of digging muscles in an Australian marsupial (*Isoodon fusciventer*). *Journal of Morphology*, *280*, 423–435. https://doi.org/10.1002/jmor.20954

McCabe, K., Henderson, K., Pantinople, J., Richards, H. L., & Milne, N. (2017). Curvature reduces bending strains in the quokka femur. *PeerJ*, *5*, e3100. https://doi.org/10.7717/peerj.3100

Milne, N., Vizcaíno, S. F., & Fernicola, J. C. (2009). A 3D geometric morphometric analysis of digging ability in the extant and fossil cingulate humerus. *Journal of Zoology*, *278*(1), 48–56. https://doi.org/10.1111/j.1469-7998.2008.00548.x

Moore, A. L., Budny, J. E., Russell, A. P., & Butcher, M. T. (2013). Architectural specialization of the intrinsic thoracic limb musculature of the American badger (*Taxidea taxus*). *Journal of Morphology*, *274*(1), 35–48. https://doi.org/10.1002/jmor.20074

Myatt, J. P., Crompton, R. H., Payne-Davis, R. C., Vereecke, E. E., Isler, K., Savage, R., … Thorpe, S. K. S. (2012). Functional adaptations in the forelimb muscles of non-human great apes. *Journal of Anatomy*, *220*(1), 13–28. https://doi.org/10.1111/j.1469-7580.2011.01443.x

Noback, M. L., & Harvati, K. (2015). Covariation in the human masticatory apparatus. *The Anatomical Record*, *298*(1), 64–84. https://doi.org/10.1002/ar.23067

R Development Core Team. (2018). *R: A language and environment for statistical computing*. Retrieved from http://www.R-project.org/.

Rohlf, F. J., & Corti, M. (2000). Use of two-block partial least-squares to study covariation in shape. *Systematic Biology*, *49*(4), 740–753. https://doi.org/10.1080/106351500750049806

Rohlf, F. J., & Slice, D. (1990). Extensions of the procrustes method for the optimal superimposition of landmarks. *Systematic Biology*, *39*(1), 40–59. https://doi.org/10.2307/2992207

Rose, J., Moore, A., Russell, A., & Butcher, M. (2014). Functional osteology of the forelimb digging apparatus of badgers. *Journal of Mammalogy*, *95*(3), 543–558. https://doi.org/10.1644/13-mamm-a-174

Salton, J. A., & Sargis, E. J. (2008). Evolutionary morphology of the Tenrecoidea (Mammalia) carpal complex. *Biological Journal of the Linnean Society*, *93*(2), 267–288. https://doi.org/10.1111/j.1095-8312.2007.00908.x

Sella-Tunis, T., Pokhojaev, A., Sarig, R., O'Higgins, P., & May, H. (2018). Human mandibular shape is associated with masticatory muscle force. *Scientific Reports*, *8*(1), 6042. https://doi.org/10.1038/s41598-018-24293-3

Sesoko, N. F., Rahal, S. C., Bortolini, Z., de Souza, L. P., Vulcano, L. C., Monteiro, F. O. B., & Teixeira, C. R. (2015). Skeletal morphology of the forelimb of *Myrmecophaga tridactyla*. *Journal of Zoo and Wildlife Medicine*, *46*(4), 713–722. https://doi.org/10.1638/2013-0102.1

Thorpe, S. K. S., Crompton, R. H., Gunther, M. M., Ker, R. F., & McNeill, A. R. (1999). Dimensions and moment arms of the hind- and forelimb muscles of common chimpanzees (*Pan troglodytes*). *American Journal of Physical Anthropology*, *110*(2), 179–199. https://doi.org/10.1002/(SICI)1096-8644(199910)110:2<179::AID-AJPA5>3.0.CO;2-Z

Travouillon, K. J., & Phillips, M. J. (2018). Total evidence analysis of the phylogenetic relationships of bandicoots and bilbies (Marsupialia: Peramelemorphia): Reassessment of two species and description of a new species. *Zootaxa*, *4378*(2), 224–256. https://doi.org/10.11646/zootaxa.4378.2.3

Vizcaíno, S., & Milne, N. (2002). Structure and function in armadillo limbs (Mammalia: Xenarthra: Dasypodidae). *Journal of Zoology*, *257*(1), 117–127.

Vizcaíno, S. F., Farina, R. A., & Mazzetta, G. V. (1999). Ulnar dimensions and fossoriality in armadillos. *Acta Theriologica*, *44*, 309–320.

Warburton, N. (2006). Functional morphology of marsupial moles (Marsupialia: Notoryctidae). *Verhandlungen Des Naturwissenschaftlichen Vereins in Hamburg*, *42*, 39–149.

Warburton, N. M., Grégoire, L., Jacques, S., & Flandrin, C. (2013). Adaptations for digging in the forelimb muscle anatomy of the southern brown bandicoot (*Isoodon obesulus*) and bilby (*Macrotis lagotis*). *Australian Journal of Zoology*, *61*(5), 402–419. https://doi.org/10.1071/ZO13086

Warburton, N. M., & Travouillon, K. J. (2016). The biology and palaeontology of the Peramelemorphia: A review of current knowledge and future research directions. *Australian Journal of Zoology*, *64*, 151–182. https://doi.org/10.1071/ZO16003

Wiley, D. F., Amenta, N., Alcantara, D. A., Ghosh, D., Kil, Y. J., Delson, E., Harcourt-Smith, W., Rohlf, F. J., St John, K., & Hamann, B. (2005,). *Evolutionary morphing*. Paper presented at the VIS 05. IEEE visualization, Minneapolis, MN.

Williams, S. B., Wilson, A. M., Rhodes, L., Andrews, J., & Payne, R. C. (2008). Functional anatomy and muscle moment arms of the pelvic limb of an elite sprinting athlete: The racing greyhound (*Canis familiaris*). *Journal of Anatomy*, *213*(4), 361–372. https://doi.org/10.1111/j.1469-7580.2008.00961.x

Zelditch, M. L., Swiderski, D. L., & Sheets, H. D. (2004). *Geometric morphometrics for biologists: A primer*. New York, NY: Academic Press.

Zelditch, M. L., Swiderski, D. L., & Sheets, H. D. (2012). *Geometric morphometrics for biologists: A primer* (2nd ed.). Amsterdam: Elsevier.

SUPPORTING INFORMATION

Additional supporting information may be found online in the Supporting Information section at the end of this article.

How to cite this article: Martin ML, Travouillon KJ, Sherratt E, Fleming PA, Warburton NM. Covariation between forelimb muscle anatomy and bone shape in an Australian scratch-digging marsupial: Comparison of morphometric methods. *Journal of Morphology*. 2019;1–16. https://doi.org/10.1002/jmor.21074